

Surface finish requirements for soft x-ray mirrors

D. L. Windt, W. K. Waskiewicz, and J. E. Griffith

We have examined the correlations between direct surface-finish metrology techniques and normal-incidence, soft x-ray reflectance measurements of highly polished x-ray multilayer mirrors. We find that, to maintain high reflectance, the rms surface roughness of these mirrors must be less than $\sim 1 \text{ \AA}$ over the range of spatial frequencies extending approximately from 1 to $100 \mu\text{m}^{-1}$ (i.e., spatial wavelengths from 1 μm to 10 nm). This range of spatial frequencies is accessible directly only through scanning-probe metrology. Because the surface-finish Fourier spectrum of such highly polished mirrors is described approximately by an inverse power law (unlike a conventional surface), bandwidth-limited rms roughness values measured with instruments that are sensitive to only lower spatial frequencies (i.e., optical or stylus profilers) are generally uncorrelated with the soft x-ray reflectance and can lead to erroneous conclusions regarding the expected performance of substrates for x-ray mirrors.

Key words: Surface finish, x-ray mirrors, multilayers, soft x-rays.

Introduction

Soft x-ray projection lithography (SXPL) is considered to be a likely candidate for the mass production of integrated circuits having 0.1- μm design rules. By using short-wavelength radiation, nominally 14 nm, coupled with low-numerical-aperture objectives (e.g., N.A. ≤ 0.1), it is possible to develop reduction-imaging SXPL exposure tools that achieve both high resolution and an acceptable depth of focus (e.g., $\pm 0.5 \mu\text{m}$).¹ Such imaging systems are all-reflective, and so they require the use of multilayer x-ray mirrors, as there are no materials available at present that could be used to make soft x-ray lenses or single-layer reflective coatings. Although the feasibility of the SXPL concept has already been demonstrated in experiments in which simple imaging systems were used, in order to produce a practical exposure tool, that is, a tool having an aberration-corrected image field large enough to fabricate large-area integrated circuits it will be necessary to develop large-diameter, diffraction-limited x-ray mirrors.

The performance requirements of the x-ray mirrors for SXPL include stringent requirements for the surface finish of the substrates, since excessive substrate surface roughness results in reduced reflectance,

which reduces the throughput (i.e., wafers per hour) of the exposure tool. For example, the efficiency of the optical system includes a term that scales approximately as R^n , where R is the peak reflectance and n is the number of normal-incidence reflections in the system. Including the illumination-system optics, the reflection mask, and the imaging-system optics, there may be as many as seven normal-incidence reflections in a commercial SXPL tool, so that a reflectance loss of 10% per mirror would result in a 52% reduction in wafer throughput.

The techniques for fabrication of the large-area mirrors required for a commercial SXPL exposure tool are now being developed. As part of this development process, it is first necessary to quantify the surface-finish requirements of the mirror substrates accurately and then to identify the surface-finish metrology tools that can be used by the manufacturer during the substrate fabrication process. The purpose of this paper is to address these issues. To this end we present results obtained in our investigation of the relationships between substrate surface finish and soft x-ray reflectance of multilayer-coated x-ray mirrors. We include brief discussions of surface-finish characterization and the relationship between surface finish and specular reflectance in the soft x-ray region, followed by experimental results that illustrate these relationships.

Surface Finish Measurement

Surface finish, that is, the fine-scale fluctuations in the effective surface height $Z(x, y)$, is best described in statistical terms. Most useful is the power spectral

The authors are with the AT&T Bell Laboratories, Room 1D-456, 600 Mountain Avenue, Murray Hill, New Jersey 07974-2070.

Received 14 April 1993, revised manuscript received 27 August 1993.

0003-6935/94/102025-07\$06.00/0.

© 1994 Optical Society of America.

density (PSD) function, $S(\mathbf{f})$, given by²

$$S(f_x) = \lim_{L \rightarrow \infty} \left(\frac{2}{L} \left| \int_{-L/2}^{+L/2} dx Z(x) \exp(-i2\pi f_x x) \right|^2 \right) \quad (1)$$

for the one-dimensional case, which describes the Fourier spectrum of $Z(x)$. Conventional surfaces [i.e., those for which $S(\mathbf{f})$ is analytic] can also be described in terms of their intrinsic surface-finish parameters σ , the rms surface roughness, and the correlation length l . These parameters are related to the power spectrum through

$$\sigma^2 = \int_0^\infty df_x S(f_x), \quad (2)$$

$$l = \frac{1}{2\sigma^4} \int_0^\infty df_x S^2(f_x). \quad (3)$$

However, as pointed out by Church,² highly polished optical surfaces (such as x-ray mirror substrates) are frequently fractallike (i.e., nonconventional), with power spectra given by inverse power laws of the form

$$S(f_x) = K_n / f_x^n. \quad (4)$$

The intrinsic surface parameters for such surfaces are then K and n , rather than σ and l , because the latter parameters are ill defined [i.e., Eqs. (2) and (3) diverge]. However, because all practical surface-finish measurement techniques are sensitive to only a finite range of spatial frequencies (i.e., they are bandwidth limited), it is always possible to measure a value for the rms roughness of a fractal optical surface, but the value measured will depend sensitively on the measurement technique used. That is, for a bandwidth-limited surface-finish measurement the rms surface roughness would be given by Eq. (2), except that the integral would be computed only over the range of spatial frequencies to which the measurement was sensitive. Thus surface-finish measurements of a fractal surface that are performed with different surface-finish metrology tools will produce different σ values, in general. For fractal surfaces (such as x-ray mirrors), therefore, specification of σ and/or l is meaningless without also specifying the spatial frequency bandpass to which these values refer.

Surface finish can be measured quantitatively by a variety of direct and indirect techniques.³ Direct metrology tools include commercially available stylus profilers (such as the Alpha-Step, Dektak, and Taly-step instruments), optical profilers (such as the WYKO TOPO and Zygo Maxim instruments) and, more recently, scanning-probe microscopes [such as the scanning tunneling microscope and the atomic force microscope (AFM)]. Each of these instruments is sensitive to a specific, finite range of spatial frequencies. Indirect surface-finish metrology techniques are simply scattering measurements of one form or

another, such as total integrated scattering and angle-resolved scattering. These measurements, too, are sensitive only to a specific, finite range of spatial frequencies; the range of spatial frequencies will depend on the photon wavelength and the measurement geometry. Since our objective is to identify the direct surface-finish metrology techniques or instruments that can be used by the manufacturer to predict the specular reflectance of an x-ray mirror, it is necessary first to identify the range of spatial frequencies that affect soft x-ray reflectance and then to select the direct metrology tools that best overlap with this spatial frequency range.

Relationship between Surface Finish and Soft X-Ray Reflectance

The specular reflectance of an optical surface depends on, among other things, the surface finish of the substrate. Simply stated, increased surface roughness will reduce the amount of light reflected in the specular direction. For scattering from an optical surface, the distribution of scattered light is directly related to the PSD through

$$dP(\theta, \phi)/d\Omega = (16\pi^2/\lambda^4)C(\theta, \phi)S(\mathbf{f}), \quad (5)$$

where $dP(\theta, \phi)/d\Omega$ is the differential fraction of incident energy per unit solid angle scattered in the direction (θ, ϕ) and $C(\theta, \phi)$ depends on the optical properties of the surface, the photon wavelength λ , the polarization of the incident and the scattered light, and the angle of incidence.⁴

For the scattering of x-rays from a multilayer-coated optical surface, the situation is more complicated, because scattering occurs not just at a single surface but at each interface in the multilayer. Nonetheless, it is possible to develop an expression for the nonspecular x-ray scattering from a multilayer structure, analogous to Eq. (5), as was presented recently by Stearns.⁵ In Stearns's model, the product $C(\theta, \phi)S(\mathbf{f})$ in Eq. (5) is replaced by a sum of equivalent products; the sum ranges over each interface in the multilayer, and each term in the sum includes a factor corresponding to the power spectrum at that interface. In general the roughness power spectrum at each interface will include contributions from both the intrinsic interfacial roughness resulting from the film growth process and the extrinsic or correlated roughness, that is, interfacial roughness resulting from replication of roughness from the underlying layers and the substrate. Both types of interfacial roughness will result in increased nonspecular scattering and, therefore, reduced reflectance. However, according to Stearns's model, correlated roughness should also manifest itself as enhanced x-ray scattering into the otherwise forbidden quasi-Bragg orders. Indeed, such nonspecular scattering has been observed experimentally.^{6,7}

We can estimate the range of spatial frequencies that will reduce the specular reflectance of an x-ray mirror by considering that each Fourier component

of the surface roughness will scatter light according to the diffraction grating equation. The amount of light scattered by a particular Fourier component (which is proportional to the magnitude of the PSD at that spatial frequency) can then be computed with Eq. (5) for a single-layer reflection or with the analogous expression for a multilayer structure as presented by Stearns. We are most interested in the specular reflectance of x-ray mirrors used near normal incidence, but the following discussion can easily be extended for nonnormal-incidence applications as well.

The diffraction grating equation is given by $m\lambda = d(\sin \alpha + \sin \beta_m)$, where m is the diffraction order, d is the grating period, and α and β_m are the angles of incidence and diffraction, respectively. For near-normal incidence ($\alpha \cong 0$) the highest spatial frequency that can reduce the specular reflectance corresponds to the condition of the scattered light just passing along the surface of the mirror; that is, $\beta = 90^\circ$. Considering only the first diffraction order ($m = \pm 1$), we have $f_{\max} = 1/d_{\min} \cong 1/\lambda$. The lowest spatial frequency of interest is in principle infinite but in practice depends on precisely how the specular reflectance is measured. For a typical reflectance measurement, in which the sample is illuminated with a pencil beam of x-rays and the specularly reflected light is collected with an electronic detector, the lowest spatial frequency will be defined by the collection angle of the detector. That is, nonspecular light scattered at angles small enough to be collected by the detector will be indistinguishable from the specularly reflected light. Thus, if the detector subtends an angle θ_{det} , the lowest spatial frequency of interest will be given by $f_{\min} = 1/d_{\max} = \sin(\theta_{\text{det}}/2)/\lambda$.

To illustrate, for the specular reflectance measurements described below, the detector subtends an angle of 2.3° in the plane of incidence, so for a normal-incidence reflectance measurement at $\lambda = 14$ nm, the spatial frequencies that can reduce the measured reflectance range from 1.4 to $71 \mu\text{m}^{-1}$ (i.e., spatial wavelengths from $0.7 \mu\text{m}$ to 14 nm).⁸ This range of spatial frequencies is largely inaccessible by most of the direct surface-finish metrology instruments listed in the previous section, with the notable exception of the scanning-probe microscopes. These instruments are ideally suited for measurement of surface finish in this range (provided that care is taken to minimize possible systematic errors).⁹

Example: Measurement of Surface Finish and Soft X-Ray Reflectance

To illustrate the ideas described above, we present here the results of our investigations aimed at relating two direct surface-finish metrology techniques with specular reflectance measurements of multilayer-coated x-ray mirrors. We have deposited high-quality Mo/Si multilayer coatings onto a variety of polished mirror substrates and have measured the

surface finish of these mirrors by the use of both an AFM and a WYKO TOPO-3D optical profiler. From these surface-finish measurements we have calculated one-dimensional PSD functions and (bandwidth-limited) rms roughnesses and have attempted to correlate these data with specular reflectance measurements made with a high-precision soft x-ray reflectometer.

Sample Preparation

A variety of highly polished optical substrates were obtained from several different commercial suppliers. The substrate materials that were investigated include single-crystal silicon and three types of high-quality glass or glass-ceramics: fused silica, Zerodur, and ULE. Polished samples of each type of glass were obtained from multiple suppliers; each supplier presumably used a different polishing technique, although no information regarding the details of the polishing processes was obtained. As the intent of our investigation is neither to compare the polishing techniques of competing optics manufacturers nor to compare the extent to which different substrate materials are polishable, but rather to determine if it is possible to correlate direct surface-finish metrology techniques with soft x-ray reflectance, we do not identify materials and suppliers in the results presented below.

Multilayer coatings consisting of 40 bilayers of Mo/Si were deposited by the use of dc magnetron sputtering in argon (3 mTorr). Substrates were mounted face down on a platen mechanism that rotated the substrates in a horizontal plane over each of two elemental sputter sources sequentially. One bilayer was deposited per rotation period. The platen itself was spun to improve the coating uniformity across the surface of each substrate. Each bilayer contained approximately 40 \AA of amorphous Si and 33 \AA of polycrystalline Mo, for a total bilayer period of

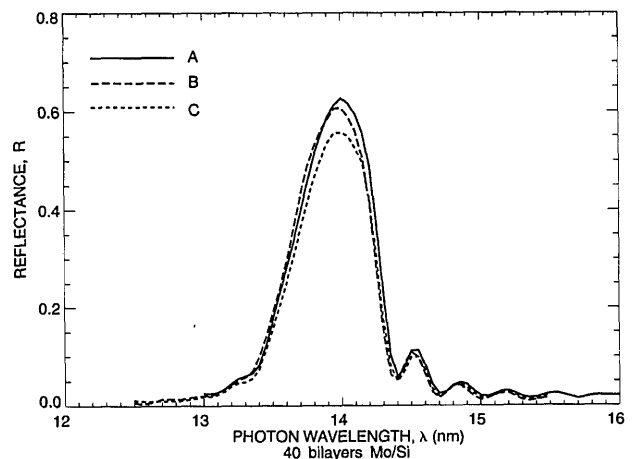


Fig. 1. Normal-incidence reflectance scans of three multilayer x-ray mirrors. All samples were coated during the same deposition run with 40 bilayers of Mo/Si, so any differences in the reflectance curves are presumed to be due to differences in the surface finish of the substrates.

approximately 73 Å, resulting in a reflectance peak centered near $\lambda = 14$ nm at an incidence angle of 3° . It should be noted that the Mo-Si interfaces in these multilayers are not sharp but have been shown previously to consist of amorphous interlayer regions of mixed composition. The presence of these diffuse interlayer regions reduces the specular reflectance by approximately 10% from what would be obtained with perfectly sharp interfaces. Indeed, this interfacial diffuseness was revealed to be the major cause for reduced reflectance in Mo/Si multilayers; the intrinsic interfacial roughness is extremely small for these structures.¹⁰

Surface-Finish Measurements

The surface finish of both coated and uncoated substrates was measured with both an AFM and a WYKO TOPO-3D optical profiler. The AFM, developed at AT&T Bell Laboratories, is based on a rocking-beam

force-balance technique.¹¹ A tungsten probe tip sharpened by a focused ion beam to a cone angle of 10° and an end radius of approximately 10 nm was used.¹² Such sharp tips are required for high accuracy up to the highest spatial frequencies examined.^{13,14} Surface-profile scans consisted of 200 scan lines \times 200 points per line, with either 5- or 10-nm steps, corresponding to scan lengths of either 1 or 2 μm . The TOPO measurements were made with both $20\times$ and $40\times$ magnification objectives, corresponding to spatial wavelength coverage ranging from 2 to 438 μm and 1 to 219 μm , respectively.

We computed one-dimensional PSD functions from the profile data, using a discrete Fourier-transform algorithm; we obtained smooth curves by averaging the PSD's computed from each scan line (or from each row of data in the case of the TOPO measurements.) We computed values for the bandwidth-limited rms surface roughness from the PSD data by the use of Eq. (2).

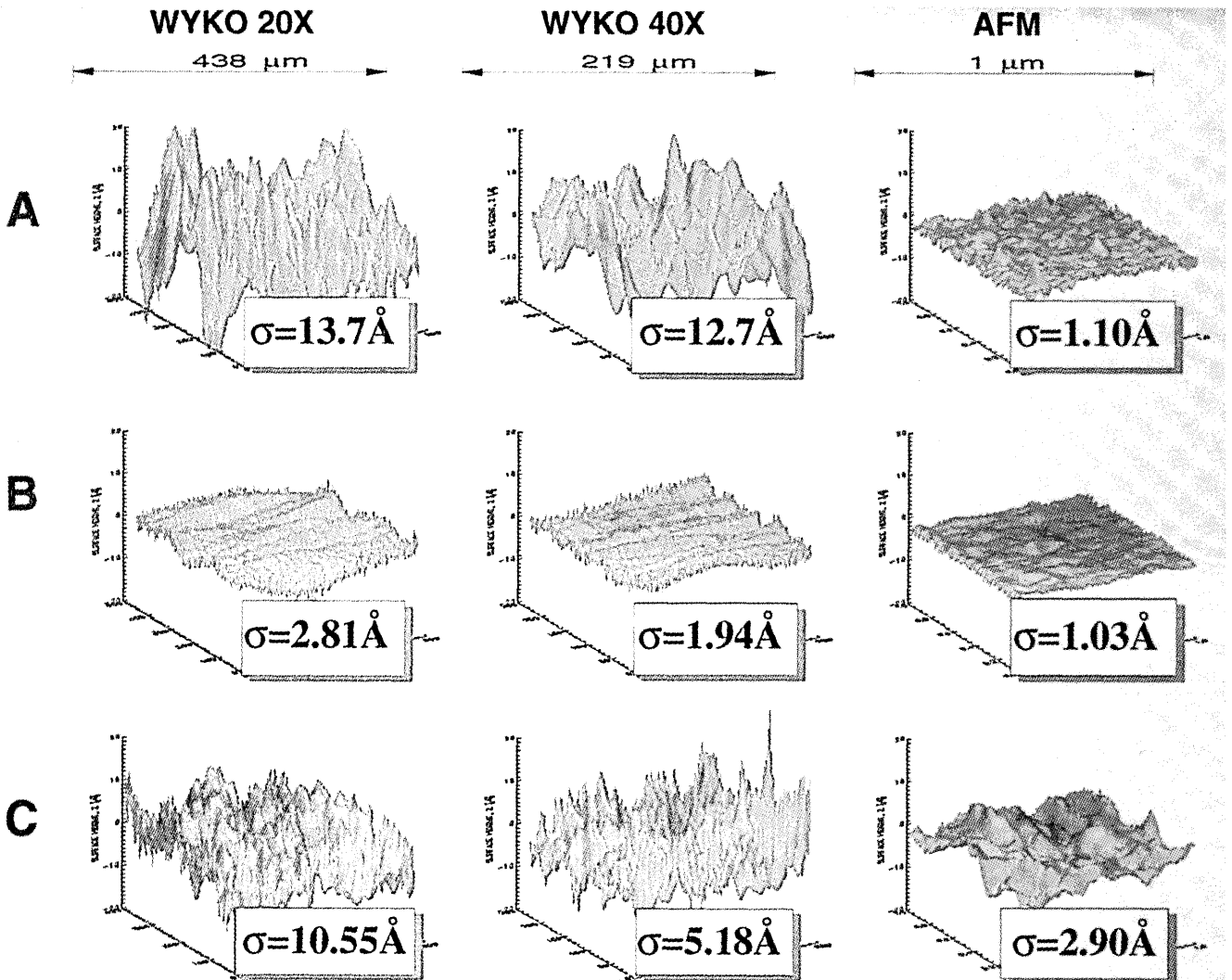


Fig. 2. Surface-height data for the three samples shown in Fig. 1. Top row, sample A; middle row, sample B; bottom row, sample C; left column, WYKO TOPO-3D, $20\times$ magnification; middle column, WYKO TOPO-3D, $40\times$ magnification; right column, AFM, 1- μm scan length. Note that the vertical scales are the same in all cases to emphasize intrinsic differences in the samples over different spatial frequency bandwidths.

Soft X-Ray Reflectance Measurements

Soft x-ray reflectance measurements of multilayer-coated x-ray mirrors were made with a high-precision, laser-plasma-based reflectometer that has been described previously.¹⁵ For the results presented below, x-ray intensity measurements of the incident and reflected beams were made with a Si diode detector having an active area of $1\text{ cm} \times 1\text{ cm}$, and the size of the beam was approximately $1\text{ mm} \times 1\text{ mm}$. The grating monochromator was configured with $100\text{-}\mu\text{m}$ entrance and exit slits, and a $1\text{-}\mu\text{m}$ -thick Be filter was used to eliminate higher-order light. Reflectance versus wavelength measurements were made at a fixed incidence angle of 3° .

Results and Discussion

In Fig. 1 we show the reflectance versus wavelength scans obtained for three exemplary samples. All three samples were coated during the same deposition run, so any differences in the reflectance curves are presumed to be due to differences in the surface finish of the substrates. In Fig. 2 we show the surface-finish measurements made after multilayer deposition for these three samples, and in Fig. 3 we show the PSD functions corresponding to the surface-height data shown in Fig. 2. For each sample, four PSD functions are shown in Fig. 3, corresponding to the two TOPO measurements ($20\times$ and $40\times$) and the two AFM scans ($1\text{-}\mu\text{m}$ and $2\text{-}\mu\text{m}$ scan lengths; the $2\text{-}\mu\text{m}$ -scan-length AFM data are not shown in Fig. 2). We obtained straight-line fits to the data shown in Fig. 3 (not shown) to estimate the fractal parameters n and K_n . The values so obtained are $n = 1.74$, $K_n = 1.3 \times 10^{-9} \mu\text{m}^{3-n}$ for sample A, $n = 1.66$, $K_n = 1.1 \times 10^{-9} \mu\text{m}^{3-n}$ for sample B, and $n = 1.74$, $K_n = 1.3 \times 10^{-9} \mu\text{m}^{3-n}$ for sample C; these values are reasonable for highly polished optical surfaces.² The peak reflectance and the values for the rms surface roughness σ computed from the PSD data are indicated in Table 1. The σ values are also indicated in Fig. 2.

As indicated in Table 1, samples A and B have the highest peak reflectances— $62.5 \pm 1.0\%$ and $60.8 \pm 1.0\%$, respectively—whereas sample C yields only

Table 1. RMS Surface Roughness and Peak Reflectance Computed from PSD Data

Sample	AFM RMS Roughness (\AA)		TOPO RMS Roughness (\AA)		Soft X-Ray Reflectance
	5 nm– 1 μm	10 nm– 2 μm	1– 219 μm	2– 438 μm	
A	1.10	1.06	12.73	13.73	$62.5 \pm 1.0\%$
B	1.03	1.02	1.94	2.81	$60.8 \pm 1.0\%$
C	2.90	2.49	5.18	10.55	$56.0 \pm 0.9\%$

$56.0 \pm 0.9\%$ reflectance, a value that is significantly lower than the other two, suggesting that sample C has greater surface roughness. Indeed, the rms roughness values for sample C obtained with the AFM, indicated in Table 1, are nearly three times the values obtained for samples A and B. Further examination of Figs. 2 and 3 reveals that the surface-height data and PSD functions for samples A and B are very similar over the range of spatial frequencies spanned by the AFM, whereas the surface-height data and the PSD function for sample C show significantly more power in the range from 0.5 to $10\ \mu\text{m}^{-1}$. In contrast, there is no correlation between the surface-finish data measured at lower spatial frequencies (i.e., those spanned by the Wyko TOPO instrument) and the soft x-ray reflectance. In particular, the low-frequency rms roughness of sample A is approximately $13\ \text{\AA}$ even though this sample has the highest reflectance.¹⁶ From these results, therefore, we conclude that, for high reflectance, the rms roughness of the substrate must be less than approximately $1\ \text{\AA}$ over the range of spatial frequencies extending approximately from 1 to $100\ \mu\text{m}^{-1}$.

In order to determine whether surface-finish measurements made on coated substrates were significantly different from those made on uncoated substrates, we used special masks during the deposition process to deposit multilayer coatings over only one half of the surface of large-diameter (50-mm) substrates. Surface-finish measurements were then made over both the coated and uncoated regions of the same sample. From these experiments we found that the presence of the coating generally had little or no effect on the measured surface finish. For example, in Fig. 4 we show the PSD functions for two regions of an extremely rough substrate (the soft x-ray reflectance of the coated portion of this substrate was only $37 \pm 0.6\%$), with one region corresponding to the bare portion of the substrate and the other to the coated portion. As can be seen from Fig. 4, the PSD functions are essentially identical. (Some high-frequency filtering was applied to the AFM data in this case to illustrate the high-frequency behavior of the PSD functions more clearly.)

According to a recently developed model for thin-film growth,¹⁷ for x-ray multilayers deposited by sputtering onto rough substrates, such as the Mo/Si multilayers investigated here, we should expect that for spatial frequencies below some cutoff value the

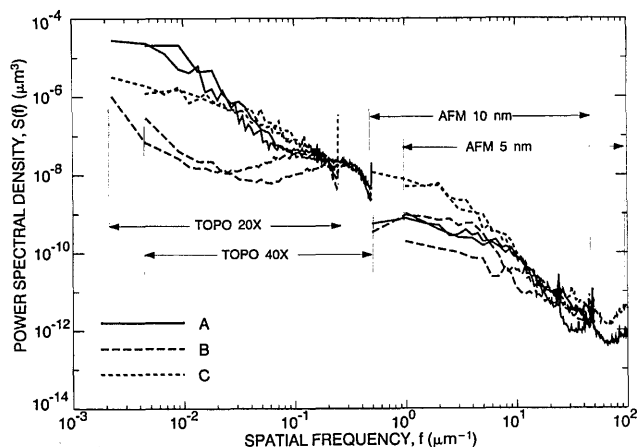


Fig. 3. PSD functions for samples A, B, and C shown in Fig. 1.

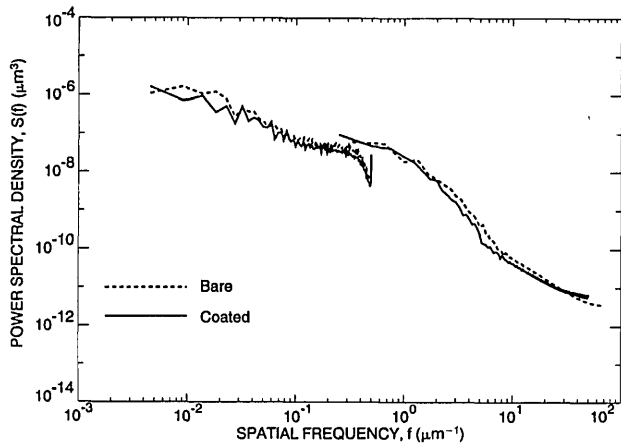


Fig. 4. PSD functions for two portions of a single substrate; one portion was coated with a Mo/Si multilayer.

roughness of the substrate will propagate through the multilayer stack during growth, resulting in (partially) correlated interfacial roughness and therefore in reduced reflectance and enhanced quasi-Bragg scattering. Above this cutoff frequency, the interfacial power spectrum will be dominated by intrinsic roughness, which is uncorrelated. The value of the cutoff frequency depends on the details of the growth process. The data shown in Fig. 4 suggest that the high-frequency cutoff for correlated roughness propagation in Mo/Si multilayers is at least as great (approximately) as the highest frequency investigated with the AFM, that is, $1/5 \text{ nm}^{-1}$.

To confirm the presence of partially correlated roughness, nonspecular x-ray scattering measurements were made for the three samples (A, B, and C) described above. The scattering measurements were made using a two-circle diffractometer with a Cu K_{α} ($\lambda = 1.54 \text{ \AA}$) rotating anode source. The incidence angle was fixed at $\alpha = 89.3^{\circ}$ (0.7° grazing), corresponding to the position of the first Bragg peak, and the detector angle β was scanned. The data are presented in Fig. 5 as scattered intensity versus scattering angle, 2θ ($=\pi - \alpha - \beta$). With a detector collection angle of 0.08° , the range of spatial wavelengths that scatter light away from the specular direction in this case extends from approximately 1 \AA to 20 \mu m and includes the entire range spanned by the AFM data as well as part of the range covered by the WYKO TOPO data.

The most striking feature of the data shown in Fig. 5 is the quasi-Bragg diffraction peaks resulting from resonant nonspecular scattering that is due to correlated roughness. The intensity of these peaks is well correlated, at least qualitatively, with the PSD data (Fig. 3) for these samples. In particular, the quasi-Bragg peaks indicated in Fig. 5 result from correlated roughness having a spatial frequency of approximately 3 \mu m^{-1} ($2\theta \cong 2.6^{\circ}$); sample C shows both the greatest amount of power at this spatial frequency and the largest quasi-Bragg peak. Furthermore, at smaller scattering angles, for example, in the region between the Bragg peak and the quasi-Bragg peak,

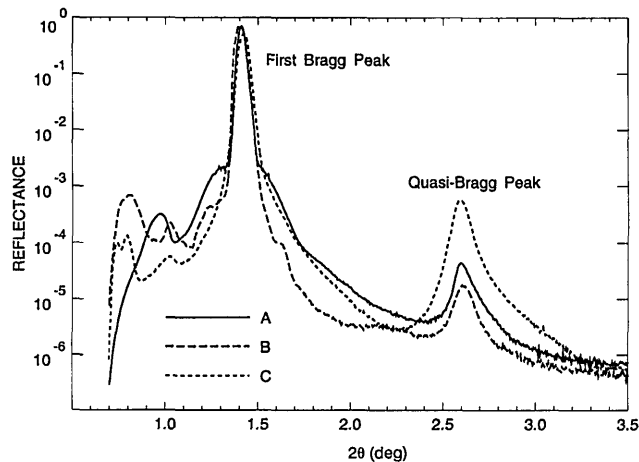


Fig. 5. Nonspecular scattering data for samples A, B, and C shown in Fig. 1. The quasi-Bragg diffraction peaks are the result of resonant scattering that is due to partially correlated interfacial roughness in the multilayer stack.

where the nonspecular intensity depends on lower spatial frequencies, the nonspecular scattered intensity is greatest for sample A, which is consistent with the rise in the PSD function for this sample at low spatial frequencies. Sample B, which is the smoothest sample over all spatial wavelengths, correspondingly shows the lowest amount of nonspecular scattered light.

Conclusion

The results presented above confirm that the peak soft x-ray reflectance of multilayer x-ray mirrors is affected by the surface finish of the substrate but only over a finite range of spatial frequencies. For Mo/Si multilayer coatings used near normal incidence at a photon wavelength of $\sim 14 \text{ nm}$, such as those being considered for use in SXPL exposure tools, this range of spatial frequencies extends from approximately 1 to 100 \mu m^{-1} (i.e., spatial wavelengths from 1 \mu m to 10 nm). This is not to say that lower spatial frequencies will not affect the performance of multilayer x-ray optics for SXPL, but to say simply that these lower spatial frequency errors will degrade the imaging quality of the optics as opposed to reducing throughput. We conclude that, for high reflectance, the rms roughness of the substrate must be less than approximately 1 \AA over the range of spatial frequencies extending approximately from 1 to 100 \mu m^{-1} .

The range of spatial frequencies that deleteriously affects the soft x-ray reflectance of multilayer optics for SXPL can be measured by scanning-probe metrology techniques, such as atomic force microscopy. The surface-finish power spectra (and the related bandwidth-limited rms surface-roughness values) of x-ray mirrors measured with an AFM were shown to correlate well with the measured specular reflectance. Furthermore, the equivalent surface-finish data obtained with an optical profiler sensitive to lower spatial frequencies (e.g., $0.001\text{--}0.5 \text{ \mu m}^{-1}$) were found to show no correlation with the soft x-ray data,

suggesting that surface-finish measurements of x-ray mirrors made with these types of instruments can lead to erroneous conclusions about the expected soft x-ray reflectance. The reason that different surface-finish metrology techniques will yield different rms surface-roughness values is that the Fourier spectrum of the surface roughness for these highly polished mirror substrates is described approximately by an inverse power law, and therefore the rms surface roughness is not an intrinsic property of the surface but rather depends sensitively on the spatial frequency bandpass of the surface-finish measurement.

We observed that the measured surface finish of x-ray mirrors was independent of whether the substrate was coated or uncoated. This implies that one can use atomic force microscopy on an uncoated mirror substrate in order to predict the soft x-ray reflectance of the substrate once it is coated with a multilayer reflector. Additionally, this result suggests that the high-frequency cutoff for correlated roughness propagation in Mo/Si multilayers is at least as great (approximately) as the highest frequency investigated with the AFM, namely, $1/5 \text{ nm}^{-1}$.

We confirmed the presence of correlated roughness by examining the nonspecular scattering from multilayer-coated substrates, which revealed the presence of quasi-Bragg diffraction peaks. The intensities of these peaks were found to be well correlated with the PSD functions for these samples.

References and Notes

1. R. R. Freeman and R. H. Stulen, "Developing a soft x-ray projection lithography tool," *AT&T Tech. J.* (November/December 1991), pp. 37-48.
2. E. L. Church, "Fractal surface finish," *Appl. Opt.* **27**, 1518-1526 (1988).
3. J. M. Bennett and L. Mattsson, *Introduction to Surface Roughness and Scattering* (Optical Society of America, Washington, D.C., 1989), Chap. 3.
4. J. M. Elson and J. M. Bennett, "Relation between the angular dependence of scattering and the statistical properties of optical surfaces," *J. Opt. Soc. Am.* **69**, 31-47 (1979).
5. D. G. Stearns, "X-ray scattering from interfacial roughness in multilayer structures," *J. Appl. Phys.* **71**, 4286-4298 (1992).
6. D. E. Savage, J. Kleiner, N. Schimke, Y.-H. Phang, T. Jankowski, J. Jacobs, R. Kariotis, and M. G. Lagally, "Determination of roughness correlations in multilayer films for x-ray mirrors," *J. Appl. Phys.* **69**, 1411-1424 (1991).
7. J. B. Kortright, T. D. Nguyen, I. M. Tidswell, and C. A. Lucas, "Substrate effects on x-ray specular reflectance and nonspecular scattering from x-ray multilayers," in *Physics of X-Ray Multilayer Structures*, Vol. 7 of 1992 OSA Technical Digest Series (Optical Society of America, Washington, D.C., 1992), pp. 102-104.
8. One is generally interested in controlling the surface of an x-ray mirror over all spatial frequencies. Low-frequency figure errors give rise to reduced image resolution, whereas high-frequency finish errors result in scattering and hence reduced reflectance. Because this work is confined to the effect of surface finish on reflectance, and because there is no universally accepted definition for the spatial frequency that separates surface figure from surface finish, here we take the pragmatic approach of defining that spatial frequency cutoff in terms of the available metrology tool, the soft x-ray reflectometer, as it is this tool that is used to measure reflectance. However, it should be noted that this cutoff is somewhat artificial, as it specifically depends on the detector collection angle used in the measurement, which is arbitrary. That is, although a detector collection angle of a few degrees is typical, small variations in this angle from instrument to instrument will result in correspondingly small variations in the long-wavelength spatial wavelength cutoff.
9. J. E. Griffith and D. A. Grigg, "Dimensional metrology with scanning probe microscopes," *Appl. Phys. Rev.* (to be published).
10. D. L. Windt, R. Hull, and W. K. Waskiewicz, "Interface imperfections in metal/Si multilayers," *J. Appl. Phys.* **71**, 2675-2678 (1992).
11. G. L. Miller, J. E. Griffith, E. R. Wagner, and D. A. Grigg, "A rocking beam electrostatic balance for the measurement of small forces," *Rev. Sci. Instrum.* **62**, 705-709 (1991).
12. M. J. Vasile, D. A. Grigg, J. E. Griffith, E. A. Fitzgerald, and P. E. Russell, "Scanning probe tips formed by focussed ion beams," *Rev. Sci. Instrum.* **62**, 2167-2171 (1991).
13. M. Stedman, "Limits of topographic measurements by the scanning tunneling and atomic force microscopes," *J. Microsc.* **152**, 611-618 (1988).
14. D. A. Grigg, J. E. Griffith, G. P. Kochanski, M. J. Vasile, and P. E. Russell, "Scanning probe metrology," in *Integrated Circuit Metrology, Inspection, and Process Control VI*, M. T. Postek, ed., *Proc. Soc. Photo-Opt. Instrum. Eng.* **1673**, 557-567 (1992).
15. D. L. Windt and W. K. Waskiewicz, "Soft x-ray reflectometry of multilayer coatings using a laser-plasma source," *Multilayer Optics for Advanced X-Ray Applications*, N. M. Ceglie, ed., *Proc. Soc. Photo-Opt. Instrum. Eng.* **1547**, 144-158 (1991).
16. Over spatial frequency regions for which the value of the PSD function (and hence the rms surface roughness) is relatively small, the intrinsic finish of the surface is masked by measurement errors, because of poor signal-to-noise ratio. The visibility of such measurement artifacts is enhanced in frequency space by the logarithmic scale, as shown in Fig. 3. Although these artifacts can be significant, in this case they are much smaller, in fact, than the inherent differences between the three samples discussed in the text.
17. D. G. Stearns, "A stochastic model for thin film growth and erosion," *J. Appl. Phys.* (to be published).